Negative Permittivity Behavior in Silver/Polyaniline Metacomposites Induced by the Low-Frequency Plasmonic Oscillation

Jiahong Tian
Shanghai Maritime University
Runhua Fan
Shanghai Maritime University
Zongxiang Wang
Shanghai Maritime University
Jiahao Xin
Shanghai Maritime University
Zhongyang Wang (zy_wang@sjtu.edu.cn)
Shanghai Jiao Tong University https://orcid.org/0000-0003-2284-8718

Research Article

Keywords: Dielectrics, Electronic materials, Plasmonics, Metamaterials

Posted Date: March 15th, 2021

DOI: https://doi.org/10.21203/rs.3.rs-239025/v1

Abstract

Silver/polyaniline (Ag/PANI) composites were prepared by an in-situ synthesis method. Interestingly, the permittivity changed from positive to negative along with the formation of percolation network. The plasma oscillations of free electrons from the network made a dominant effect on the negative permittivity behavior. Further investigation based on equivalent circuit analysis revealed that the composites with negative permittivity presented inductive character. The epsilon-negative composites can be applied to electromagnetic shielding, absorbing and attenuation.

1. Introduction

Electromagnetic metamaterials with simultaneously negative permittivity and permeability have drawn intensive attention for their exotic physical properties and widespread applications in perfect lens, invisibility cloaks, resonators, and ultrathin antennas, etc [1]. Recently, single negative materials, in which either the permittivity or permeability is negative, have also shown bright prospects in electromagnetics, especially epsilon-negative ($\varepsilon < 0$) materials exhibit fascinating performances in electromagnetic shield, field-effect transistors and high-k capacitors [2]. In metamaterials, the epsilon-negative properties are realized based on the periodical artificial structures, in which the shape, size, and configuration affect the negative permittivity [3]. Moreover, the geometry size of building blocks of metamaterials is dependent on the wavelength of electromagnetic waves. In frequency band of several MHz or even kHz, the wavelength up to few meters and even kilometers, thus it is difficult to design metamaterials with periodical building blocks of such large size [4].

In recent years, metacomposites have been widely considered for novel epsilon-negative materials [5]. The metacomposites are defined as those composites with anomalous physical properties that are uncommon in conventional materials [6]. Z. Shi et al. [7] obtained controllable negative permittivity in alumina matrix composites with nickel particles in radio frequency. Afterwards, T. Tsutaoka et al. [8] investigated the negative permittivity of polymer-matrix composites containing metallic fillers and observed the similar phenomenon. Negative permittivity in these metacomposites is in close association with materials' composition and microstructure, rather than artificial building blocks in metamaterials [9]. Thus, it provides a new approach to epsilon-negative materials with processing methods of materials science [10].

Absolutely, the appearance of negative permittivity is determined by the percolation of conductive fillers in metacomposites, while percolation is always influenced by fillers' size, geometry, and surface state [11]. Generally, one-dimensional fillers have low percolation threshold due to their high aspect ratio [12]. In addition, polymer matrix is more favorable to obtain flexible epsilon negative metacomposites, which have great potential in wearable devices [13]. Therefore, this work intends to realize negative permittivity in PANI matrix composites with silver nanowires as fillers, and thoroughly investigate their dielectric properties.

2. Experimental

2.1 Materials

P-Toluene sulfonic acid (PTSA), ammonium persulfate (APS), aniline, ethylene glycol, silver nitrate, polyvinylpyrrolidone (molecular weight ~ 30000), and sodium chloride were purchased from Sinopharm Chemical Reagent Co., Ltd (China). The aforementioned analytical reagents were used without any treatment.

2.2 Preparation of Ag/PANI composites metacomposites

A polyol method was employed to prepare Ag nanowires, which has been reported in our precious work [14]. Then, PTSA and APS were used as protonic acid and oxidant to polymerize aniline. During the synthesis, adding different mass fractions (0, 10, 15, 30 and 40 wt%) of Ag nanowires to prepare Ag/PANI composites metacomposites. The detailed polymerization process of PANI matrix composites can refer to the reported literature [15].

2.3 Characterization and measurement

The microstructure was investigated by a PANalytical X' Pert PRO X-ray diffractometer (Netherlands). The morphology of composites and Ag nanowires was observed by a Zeiss Sigma 500 field emission scanning electron microscope (Japan) and a JEM 2100F high-resolution transmission electron microscope (Japan), respectively. The electrical and dielectric properties of the samples were tested by a Keysight E4980AL LCR meter (USA).

3. Results And Discussion

Figure 1 shows the XRD pattern and morphology of Ag/PANI composites. The broad double-peak at circa 19–23° indicated the amorphous nature of PANI (Fig. 1a). The diffraction peaks corresponding to Ag can be confirmed in pure Ag, while the characteristic peaks were covered in the composites (Fig. 1a). Figure 1b showed the morphology of Ag nanowires with a large aspect ratio. However, after adding the prepared Ag nanowires to synthesize PANI, the nanowires can hardly be observed in the SEM image of Ag/PANI composites. It indicated that the nanowires were destructed by the violent stir during the synthesis of PANI, then the shortened silver were wrapped by the PANI matrix. Hence, it is difficult to observe the silver nanowires in the composites. When the content of Ag reached to 10 wt%, the neighboring Ag particles cannot completely contact with each other to establish a conductive network (shown in Fig. 1c). After the Ag content reached to 30 wt%, Ag particles interconnected and gradually constructed a percolation network (Fig. 1d).

Frequency dependence of the real part permittivity (ε_r') is shown in Fig. 2a. The largest values of ε_r' of PANI fabricated in this work reached up to 10^4, but ε_r' gradually decreased as frequency increased. When the content of Ag was 10 wt%, ε_r' of the Ag/PANI composite was greatly enhanced due to the increasing interfacial polarizations between Ag and PANI matrix. When the composites were put into an electric field,

electric charges aggregated at the heterogeneous interfaces, contributing to the enhanced permittivity. However, the decreasing tendency of ε_r' versus to frequency was more evident. The variation of ε_r' of PANI and PANI-10% Ag composites showed relaxation features and can be well fitted by Debye equation [9]:

$$\varepsilon_r' = \varepsilon_\infty + \frac{\varepsilon_s - \varepsilon_\infty}{1+\omega^2\tau^2} \quad (1)$$

where ε_∞ is the permittivity at nearly optical frequency, ε_s is the static permittivity, ω is the angular frequency and τ is the relaxation time. Dielectric relaxation occurs along with a significant decrease of permittivity, when polarization cannot keep up with the change of frequency. Further increasing the content of Ag caused a negative permittivity in Ag/PANI composites. This is attributed to the fact that electrons in the interconnected Ag paricles became delocalized in the percolating networks. Thus, the negative permittivity originated from the plasmonic state of free electrons within the composites. Furthermore, negative permittivity of free electron gas was depicted by Drude model [16]:

$$\varepsilon_r' = 1 - \frac{\omega_p^2}{\omega^2+\omega_\tau^2} \quad (2)$$

$\omega_p=(n_{eff}e^2/m_{eff}\varepsilon_0)^{1/2}$ is the plasma frequency determined by the effective mass (m_{eff}) and concentration (n_{eff}) of electrons. The experimental results agreed well with the Drude model, suggesting that the plasma-like negative permittivity is related to plasma oscillations of electrons introduced by Ag particels. Meanwhile, the magnitude of the negative permittivity was proportional to the content of Ag owing to the increase of effective electron concentration.

Figure 2b shows the reactance (Z'') spectra of Ag/PANI composites. When the content of Ag was no more than 10 wt%, Z'' was negative, indicating that the composites was electrical capacitive. When the content of Ag reached up to 15 wt%, Z'' became positive and the composites turned into electrical inductive. The spectra of Z'' were also fitted by the inserted equivalent circuit models in Fig. 2b and the fitting results also demonstrated that inductive components were employed to analyze the samples with negative permittivity. In addition, there was a relationship between ε_r' and Z'' [17]:

$$\varepsilon_r' = -\frac{Z''}{\omega C_0 (Z'^2+Z''^2)} \quad (3)$$

It suggested that the sign of ε_r' is closely related to that of Z''. Thus, the appearance of negative permittivity in the composites with high content of Ag is corresponding to the inductive character. Meanwhile, the phase relationships between electric voltage and currents were different in the composites with positive and negative permittivity. When ε_r' is positive and Z'' is negative, the current phase lags the voltage phase, while that is just reversed when ε_r' is negative and Z'' is positive.

Figure 3a shows the ac conductivity (σ_{ac}) of Ag/PANI composites with different content of Ag. σ_{ac} was almost frequency independent in low frequency region but slightly increased in high frequency region for

the composites with low content of Ag. This phenomenon was related to the hopping conduction mechanism, which depicted that the conductivity was contributed by carriers' hopping among the isolated Ag particles. When the content of Ag increased from 30–40%, σ_{ac} was greatly enhanced under the action of conductive silver networks within PANI matrix. In this case, the increased conductivity was ascribed to electrons' movements in the formed percolating pathways. Thus, as the content of Ag increased, more electrons in Ag fillers contributed to the electrical conductivity. The inserted figure in Fig. 3a shows the variation of σ_{ac} at 5 kHz versus to the mass fraction of Ag. It indicated that the conductivity of Ag/PANI composites evidently improved after incorporating Ag particles, which agreed well with the percolation theory: $\sigma \propto (f\text{-}f_c)^t$ [11]. Thus, the conduction mechanism of hopping conduction changed to metal-like conduction as the conductivity increased dramatically. Imaginary part of the complex permittivity (ε_r'') usually indicates dielectric loss in the materials. Frequency dependence of ε_r'' is shown in Fig. 3b. ε_r'' of all samples was almost inversely proportional to frequency. Taking into the measured data of σ_{ac} into the formula for conduction loss calculation: $\varepsilon_r'' = \sigma_{ac}/\omega\varepsilon_0$ [18], the calculated results were almost consistent with the measured ε_r'', which suggested that the dielectric loss of Ag/ PANI composites was mainly caused by conduction loss.

4. Conclusion

Ag/PANI composites were fabricated and the negative permittivity behavior was investigated. For the composites with low content of Ag, the permittivity was positive and the dielectric dispersion showed relaxation features. As the content of Ag increased, the permittivity became negative due to the plasma oscillations of free electrons mainly from interconnected Ag. Combined with the equivalent circuit analysis, it demonstrated that epsilon-negative materials presented electric inductive character. Herein the revelation of negative permittivity opens up an approach to metacomposites.

Declarations

Acknowledgments

The authors sincerely thank the Innovation Program of Shanghai Municipal Education Commission (2019-01-07-00-10-E00053) and Shanghai Engineering Technology Research Centre of Deep Offshore Material (19DZ2253100) for their financial supports.

References

1. D.R. Smith, W.J. Padilla, D. Vier, et al., Phys. Rev. Lett. 84 (2000) 4184-4187.
2. G. Fan, Z. Wang, Z. Wei, et al., Compos. Part A-Appl. S. 139 (2020) 106132.
3. J.B. Pendry, A.J. Holden, W.J. Stewart, et al., Phys. Rev. Lett. 76 (1996) 4773-4776.
4. W.J. Padilla, D.N. Basov, D.R. Smith, Mater. Today 9 (2006) 28-35.

5. D. Estevez, F. Qin, Y. Luo, et al., Compos. Sci. Technol. 171 (2019) 206-217.
6. Y. Luo, D. Estevez, F. Scarpa, et al., Research 2019 (2019) 3239879.
7. Z. Shi, R. Fan, Z. Zhang, et al., Adv. Mater. 24 (2012) 2349-2352.
8. T. Tsutaoka, T. Kasagi, S. Yamamoto, et al., Appl. Phys. Lett. 102 (2013) 181904.
9. G. Fan, Z. Wang, H. Ren, et al., Scr. Mater. 190 (2021) 1-6.
10. Z. Wang, K. Sun, P. Xie, et al., Acta Mater. 185 (2020) 412-419.
11. Z. Wang, K. Sun, P. Xie, et al., Compos. Sci. Technol. 188 (2020) 107969.
12. C. Nan, Y. Shen, J. Ma, Annu. Rev. Mater. Res. 40 (2010) 131-151.
13. K. Sun, J. Dong, Z. Wang, et al., J. Phys. Chem. C 123 (2019) 23635-23642.
14. K. Sun, L. Wang, Z. Wang, et al., Phys. Chem. Chem. Phys. 22 (2020) 5114-5122.
15. X. Yao, X. Kou, J. Qiu, et al., J. Phys. Chem. C 120 (2016) 4937-4944.
16. G. Fan, Z. Wang, K. Sun, et al., J. Mater. Chem. C 8 (2020) 11610-11617.
17. K. Sun, J. Xin, Y. Li, et al., J. Mater. Sci. Technol. 35 (2019) 2463-2469.
18. Y. Qing, Q. Wen, F. Luo, et al., J. Mater. Chem. C 4 (2016) 4853-4862.

Figures

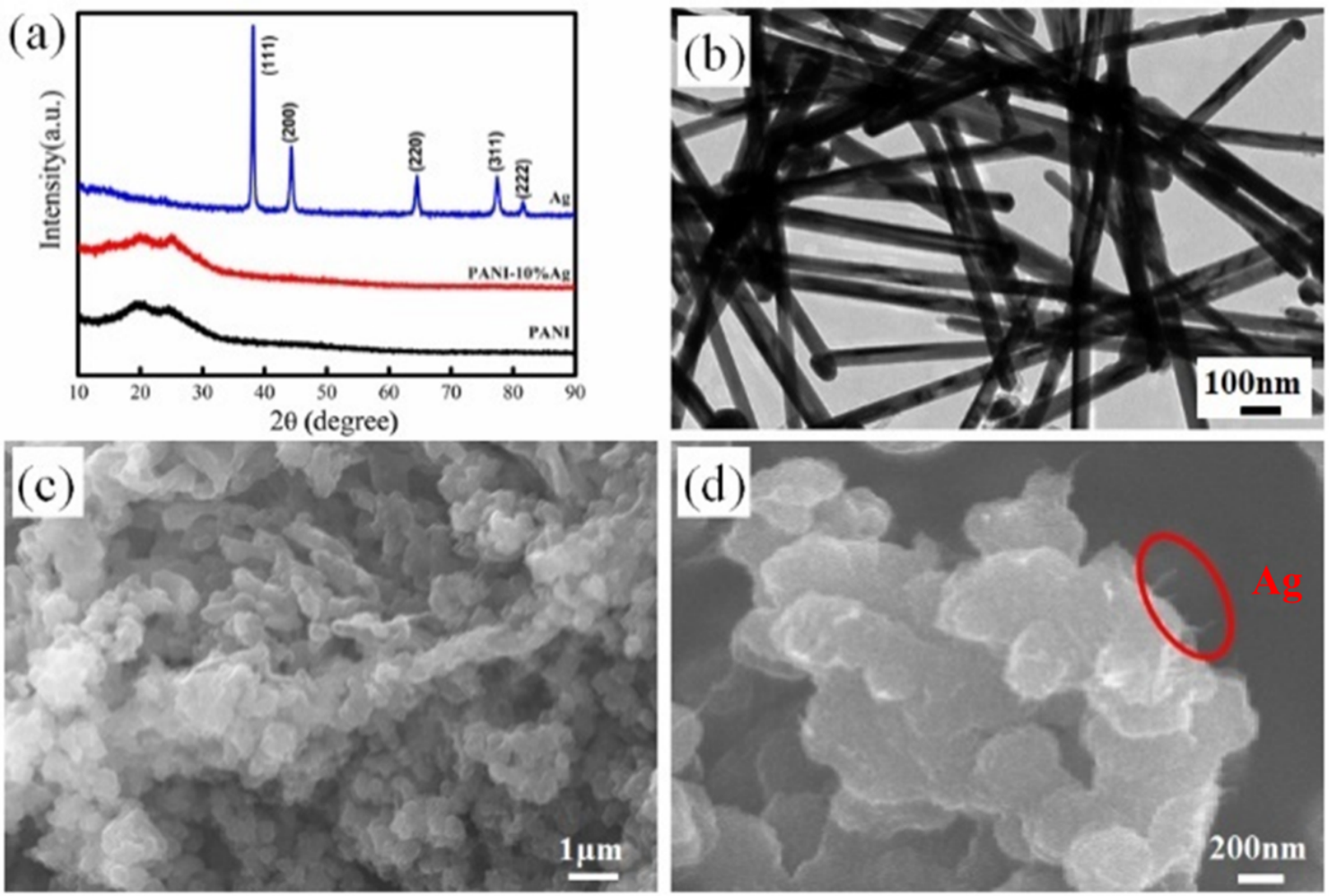

Figure 1

(a) XRD patterns of Ag nanowires, PANI, and Ag/PANI composites. (b) TEM images of Ag nanowires. (c, d) SEM images of Ag/PANI composites with different mass fractions of Ag, (c): 10%, (d): 30%.

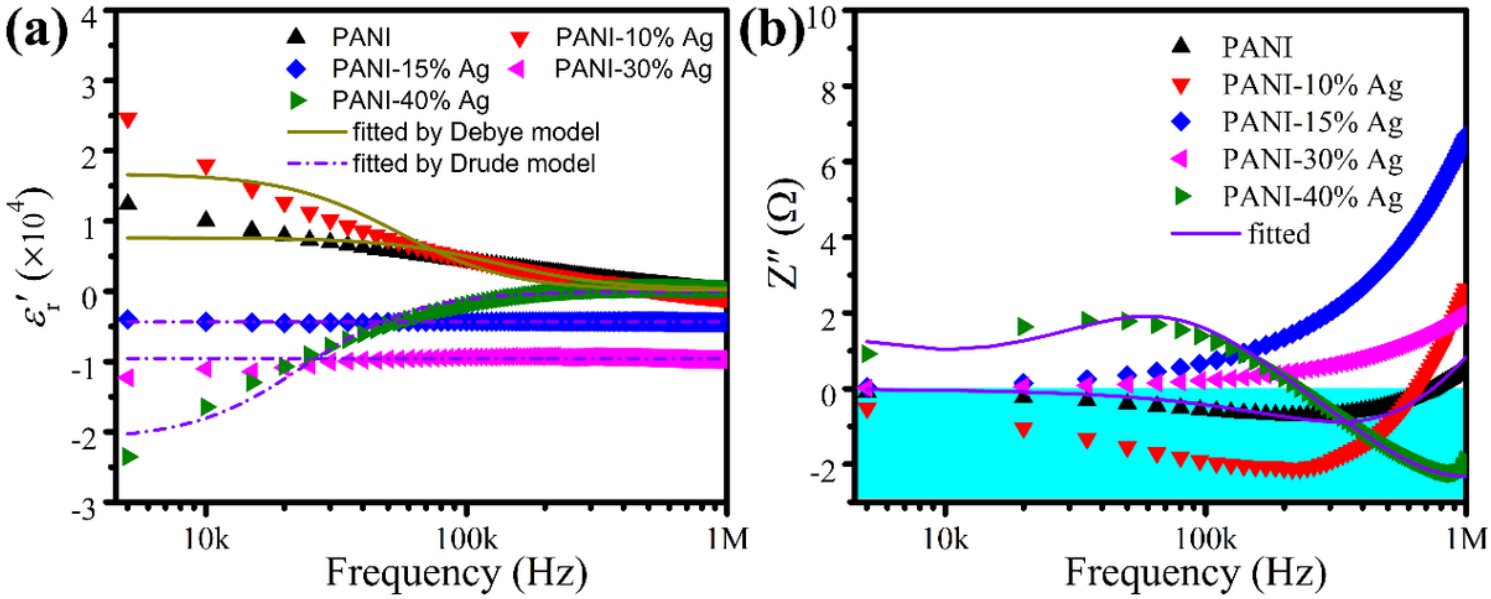

Figure 2

Frequency dependence of εr' (a) and Z" (b) of Ag/PANI composites

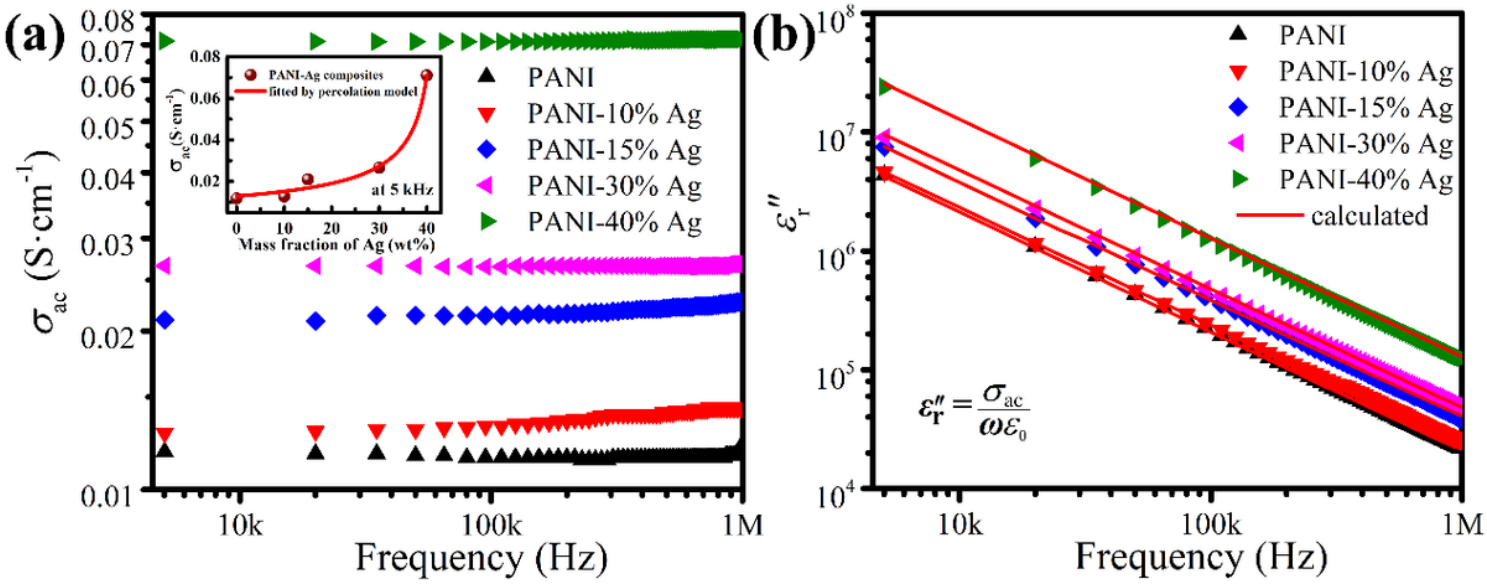

Figure 3

Frequency dependence of σac (a) and εr" (b) of Ag/PANI composites